Plantation Rows Identification by Means of Image Tiling and Hough Transform

Guilherme Afonso Soares, Daniel Duarte Abdala and Mauricio Cunha Escarpinati

Faculty of Computing, Federal University of Uberlândia, Uberlândia, Brazil

Keywords: Image Processing, Crop Lines Identification, Precision Agriculture.

Abstract: In this work we address the problem of plantation rows identification on UAV imaged coffee crop fields. A fair number of approaches address the problem using the Hough Transform. However it assumes the plantation lines are straight which is hardly the case in Aerial images. We propose a tiling scheme which allows one to acceptably approximate the rows inside each tile to straight lines making it feasible to apply the Hough Transform. Experimental results compared to ground truths seems to indicate the proposed approach successfully approximate real plantation rows.

1 INTRODUCTION

Nowadays precision agriculture is heavily dependent on imaging and mapping technologies e.g. for estimating growth (Kataoka et al., 2003), or identifying other important agronomic characteristics (Sankaran et al., 2015) such as nitrogen stress (Blackmer and Schepers, 1996). Advances in Unmanned Aerial Vehicles - UAV - technology led to its widespread popularization. With the corresponding drop in operational costs even smaller plantations are now able to afford the usage of imaging aided technologies.

The latest economic report by the Association of Unmanned Aerial Vehicle International (AUVSI, 2013) points out the agricultural market is by far the largest segment for UAVs. In the United States alone it is forecast to create thousands of new jobs and considerable revenue and taxes. With the market growth production costs are expected to drop. It in turn will allow smaller enterprises such as family and small agricultural cooperatives (Turner et al., 2016) to benefit from the diminished operational costs to also make use of precision agriculture aided by UAVs. Other countries like Japan are also making extensive use of UAVs in agriculture and in Brazil a number of startup companies such as Sensormap, Orion and Sensix to cite just a few are producing and commercializing UAVs.

There are obvious market for UAVs been agriculture the most prominent example. The technology is mature and the market offers a number of cost effective solutions. However, the market lacks reliable software to process the remote sensed data. With the dawn of UAVs to adapt solutions derived from previously used aerial vehicles would be the obvious choice. However, the available software was developed for vehicles that capture images on either high (planes and helicopters) or ultra-high (satellites) altitudes. The problem is further complicated by the fact that much of the existing software on the market is proprietary.

In this context the need of developing new software able to dealing with low or medium altitude imagery became clear. Additionally the development of new, better and cheaper imaging sensors opens new avenues of exploration.

New application niches are opening in precision agriculture aided by low/average altitude remote sensing. Among them, a key problem is to identify where the planting rows are located in the imaged field. This procedure is important for crop planning, production estimation, plant counting, harvesting and early correction of failures in sowing. Considering the imaging processing techniques available, the Hough Transform (Hough, 1962) figures as an initial clear choice. As shown in (Illingworth and Kittler, 1988) it is widely used in identifying fixed parameterized shapes formed by points on images. The basic Hough Transform works well for regular geometric forms, like straight lines and circles, but it can also be used to find arbitrary shapes (Ballard, 1981). However it requires that the object shape to be known in advance, which limits its application on plantation row tracking. It is worth notice that sometimes crops follow

the terrain, are hindered by obstacles or any other arbitrary unknown geographical feature. Nonetheless a number of solutions were proposed using the Hough Transform as basis.

In (Ronghua and Lijun, 2011) a crop row detection algorithm is presented using as basis the Hough Transform. It works on ground level images taken manually with a hand camera. In (Leemans and Destain, 2006) a row localization method is proposed in which uses an adaptation of the Hough Transform. It also works on ground level images captured by a camera mounted on a tractor. The method is specifically tunned to deal with early sowing and was tested only with chicory. In (Søgaard and Olsen, 2003) approaches the problem from a similar perspective. Since those methods operate on images captured by tractor mounted cameras, they make the assumption that plantation rows can be approximated by straight lines. In (García-Santillán et al., 2017) such approximation is not used. However, it also uses ground level images. It assumes a few properties about the images, such as the fact that there will be roughly vertical lines starting at the image bottom. It also uses a local approach, whereas this work proposes to find the lines on the whole mapped area. There are approaches for finding general curves from a set of points, as described in (Lee, 2000). These approaches require the set of points to comprise only one curve.

Differently from ground level imagery, in low to mid altitude aerial images plants are perceived as variations in green intensity and can commonly be intertwined with weed. In (Ramesh et al., 2016) a image processing procedure is presented to identify rows of tomato plants using images from a multi spectral camera mounted on a quad-copter. The images used in this study were captured in low altitude (a few meters above de ground) and there are no visible vegetation other than the plants of interest.

In dealing with coffee plantations its is very common for the plantation rows to follow natural geographical features within the field. The implication is translated in plants been sowed following curves. Previously reviewed methods based on the Hough Transform would most likely fail on such images. They were specifically designed to deal with plantation rows that can be considered straight. This is not an issue if the images were captured by a camera mounted on a tractor navigating the field. Images sensed by UAV mounted cameras are naturally more cost effective, despite the fact that the final results shows a much broader spatial resolution. The rows will be curved and the Hough Transform will fail in identifying meaningful plantation rows.

In this work we address the problem of coffee

Figure 1: Typical coffee plantation plantation following the geographical features of the field. Locally, segments of the curves can be approximated to straight lines.

plantation rows identification on images sensed by UAV mounted RBG camera from up to 100m above the plantation level. This image source impose a restriction in using the Hough Transform since the plantation lines cannot be considered straight. Similarly to previously discussed methods, the Hough Transform is the basis of our algorithm. To make it feasible the input image is first divided in a set of partially overlapped tiles. In doing so, each plantation line segment can be roughly approximated to a locally straight line, making the application of the Hough Transform feasible. Fig. 1 depicts this situation. As one can see, the plantation lines highlighted are curved. If a tile small enough is considered they can be successfully approximated to straight lines.

The main contribution of this work is the proposal of a procedure to extract from mid altitude images plantation row segments. The final result of this algorithm are sets of simple, very short lines which approximate quite precisely real plantation lines. Subsets of those lines present a high level of overlapping allowing subsequent partition and by means of interpolation procedures to extract the final plantation lines.

The remainder of this paper is organized as follows. In Section 2 the algorithm for plantation lines identification is presented. Section 3 present the experiments and a discussion of the results. Section 4 presents conclusions and possible future developments.

2 METHODS

The input data is comprised of images of coffee plantations captured by UAV mounted RGB camera flying on average at 100 meters above the plantation. The way drone sensing works a series of small images are captured and afterwards they are composed by imag-

ing mosaicking techniques into a single piece. At the end of the process a color image *I* is outputted with dimensions approximately 1800×1550 pixels. Prior to the identification of the plantation rows it is required that some preprocessing takes place in order to make it adequate for the application of the Hough Transform.

2.1 Preprocessing

Once the input image is available it has to undergo a preprocessing step in order to prepare it for the application of the Hough Transform. The aim is twofold: a) remove extraneous objects as much as possible; and b) salient the actual plants. This is accomplished by means of the following image processing pipeline.
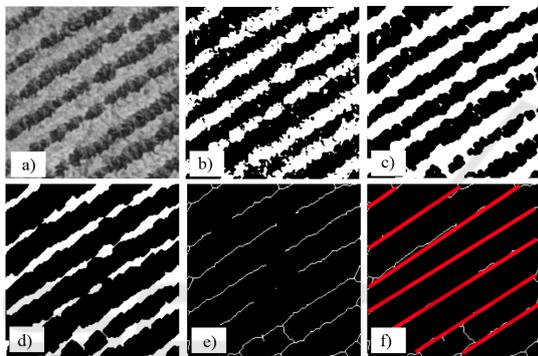

Figure 2: Processing Steps: a) Gray Level conversion; b) k-means binarization; c) Morphological Closing; d) Morphological Erosion; e) Morphological Skeleton and Pruning; f) Hough Transform.

2.1.1 Color Remapping

In this first step, the color image is remapped to gray scale. This is a simple procedure that can be accomplished by taking the arithmetic average of the three color channels, e.g. $Gray(x,y) = (R(x,y) + G(x,y) + B(x,y))/3$. Fig. 2-a shows a plantation tile after the conversion to gray scale.

2.1.2 Binarization

The grayscale image is binarized by means of a simple clustering function. The aim is to divide the image pixels into two very distinct classes: a) plants; and b) ground and extraneous objects. Due to the fact the imaging procedure can take place in a number of different atmospheric conditions simple thresholding is usually not enough to provide the needed discriminative power on this wide variation of conditions.

Firstly two centroid values are picked by inspecting the minimum and maximum pixel values of the image. The K-means algorithm is then set to run.

Eventually it outputs two classes of pixels. One of those classes is composed by the pixels of plants and the other is mostly ground and extraneous objects. Experimentally it was observed the plants cluster pertains circa 40% and the ground cluster circa 60% of the total. A simple decision rule was sufficient to decide which cluster represents the foreground and which represents the background in all images used in the experiments. The result achieved by clustering binarization can be observed in Fig. 2-b.

2.1.3 Opening & Closing

The opening of the binary image is done by the 'disk' structuring element with value 4. For a close operation a 'line' structuring element is used with the radius 4. The morphological operations are shown in Fig. 2-c and 2-d. The resulted images shows contiguous figure and all rows are separated individually.

2.1.4 Thickness Pruning

A second opening/closing convolution is used in order to eliminate discontinuities present in the image. This is accomplished by using a diamond shaped kernel of size 4. Later on, to reduce the thickness of the detected lines, a operation of skeletonization is applied, followed by a pruning algorithm. The structuring element 'Morph Cross' is used with radius 3. The skeletonized results of this process is shown in the Fig. 2-e.

At this point the image is ready to be tiled. The computation of window coordinates is tricky and therefore deserves a detailed discussion.

2.2 Input Image Subdivision

As discussed earlier the direct application of the Hough Transform to identify the plantation lines on the entire image is not feasible, once it is not capable of detecting curves. The proposed method is an alternative front of the traditional method, on which it is applied locally, using small tiles in which the segments could be accurately approximated to straight lines. Experimentally it was observed this approach indeed works. However if the windows are taken without no overlap serious discontinuities in the plantation lines will occur. Therefore we propose the tiles to be taken with some degree of superposition. Fig. 3 shows some tiling examples. In a) the tiles are taken without overlap and in b) 25% of the tile size is overlapped. In c) we observe the effect of not using tile overlap. Line segments tend to present considerable discontinuity. Finally in d) it became clear that by overlapping the tiles to some extent such discontinuities are mostly removed.
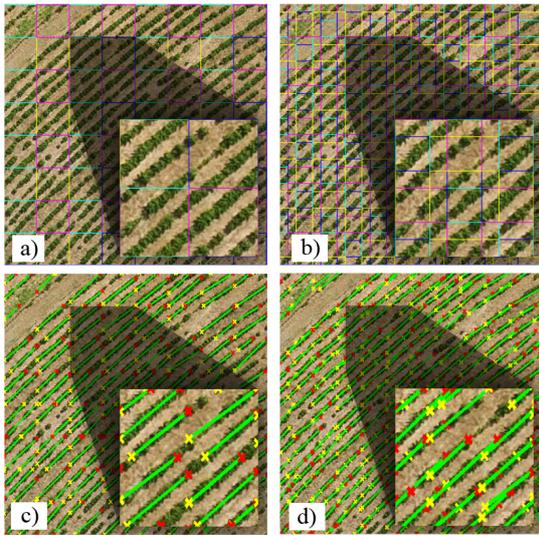
Figure 3: Overlap Strategy: a) image windowed without overlap; b) image windowed with overlap of 25%; c)Processed image windowed without overlap; d) Processed image windowed with overlap of 25%.

The computation of the tiles coordinates can be tricky. Therefore, we define two parameters. The first one β represents the size (in pixels) of the square tile. The second parameter α represents the degree of overlap desired.

$$c = \lceil \frac{w}{\beta(1-\alpha)} \rceil$$
$$r = \lceil \frac{h}{\beta(1-\alpha)} \rceil \quad (1)$$

In order to compute the coordinates of each window we first require to estimate the number of tiles in each row and column. Equation 1 specifies how to compute the number of columns - c - and rows - r - for a given image. It depends of the width - w - and height - h - of the image as well as the size of the desired window and the degree of overlap. The ceil operator is taken to ensure a round number of columns and rows since there is a possibility the mosaicking of windows will not fit perfectly inside the image. In such cases tiles located in the rightmost column and bottom row will potentially be not squared and smaller in comparison to the other tiles.

The coordinates of each tile can be computed using Equations 2. $[x_l, y_u]$ correspond to the upper left coordinate of the window and $[x_r, y_b]$ to the bottom right. Variables i and j are the row and column indexes of the windows grid over the image. The windowing strategy is depicted in Fig. 3.

$$x_l(i) = i(\beta(1-\alpha)),\ 0 \leq i \leq c$$
$$y_u(j) = j(\beta(1-\alpha)),\ 0 \leq j \leq r$$
$$x_r(i) = x_l(i) + \beta$$
$$y_b(j) = y_u(j) + \beta \quad (2)$$

A side effect of the tiling scheme is the introduction of undesired artifacts not pertaining to the plantation lines. Such artifacts can be seen as noise and therefore a post processing filtering step is required.

2.3 Hough Transform and Post Processing

Considering the coordinates of each tile, the method proceeds by applying the Hough Transform. As output, a set of lines (represented by its two end points) is returned for each tile. The line segments can be observed in Fig. 3 and 4.
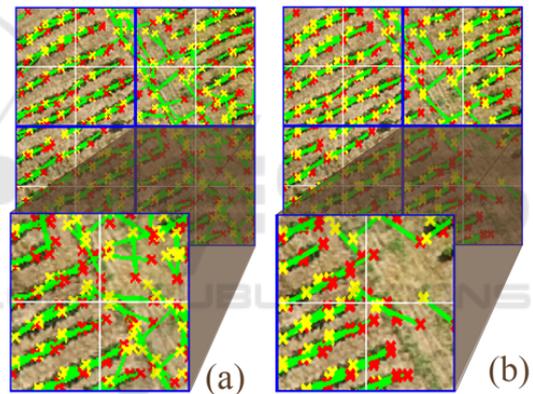

Figure 4: Denoising example with 2 as index: a) Figure without a denoising process; b) Figure with denoising algorithm.

Although the overlap strategy solves the problem of line discontinuity as side effect a number of extraneous lines are produced. Therefore some filtering is required as post processing in order to remove such undesired lines. It happens in two stages: i) inside each tile; and ii) using larger tiles with size $\gamma = \times 1.5, \times 2.0$ or $\times 2.5$ the size of the individual tiles, γ is also called denoising index. The second stage is necessary to further expunge erroneous segments. In both stages the same set of steps are taken.

The noise removal starts by computing the angular coefficient $m = \Delta_y / \Delta_x$ for all lines in a tile. All coefficients are then rounded to one decimal place. The statistical mode is then computed for the angular coefficients and it is taken as the orientation tendency for the tile. All lines are inspected for intersection and in identifying such event all lines but the one closest

to the tiles angular coefficient mode are removed. Afterwards all remaining lines are inspected with regard to the distance of its angular coefficient to the mode. Any line which differ from the mode for more than a parameter δ are also removed. The difference should be taken in absolute values. In our experiments δ was set to 0.3 whose results are shown on Fig 4.

3 DATASETS AND EXPERIMENTS

Eight distinct aerial images taken from a UAV named sx2 (fig. 5) were used in our experiments. During capture the the vehicle flies between 100 and 150 meters above the ground. It's air speed must be at least 10 meters per second, not exceeding $15m/s$. The UAV is completely autonomous and can fly up to 1.5 hours nonstop. The flight path is set to cover all analyzed area. It is also configured that a snapshot of the plantations is taken every 2 seconds. The RGB camera used to take the pictures is a modified Canon S110. Originally it can only capture red, green and blue (RGB) frequencies, however to calculate the NDVI the near-infrared spectrum is needed. Therefore, the original optical filter is replaced for one that enables the perception of the near-infrared channel, resulting in a near-infrared green and blue (NIRGB) image. For the purposes of this experiment, NIR was taken as Red channel. In order to the results comparison, the images used in the tests are available in: (http://www.facom.ufu.br/ mauricio/VISAPP2018/).

Figure 5: UAV utilized to capture crop images.

As previously presented, the proposed method depends on three main parameters: size of tiles (β), overlap percentage of (α) and denoising tile size (γ). In order to evaluate the performance of the proposed algorithm in terms of the presented parameters, tests were performed with different sets combining the values of β, α, and γ. The values used on those experiments are presented by Table 1.

To evaluate the effectiveness of the proposed

methodology, the images used were taken from different coffee plantations and submitted to the proposed algorithm. In order to assess the algorithm's accuracy under different commonly encountered conditions, the images were taken with varying terrain, atmospheric conditions and plant growth stages.

Each image had its **ground truth** manually generated by a specialist, who manually marked the intended plantation rows. After applying the proposed algorithm and obtaining a total of 36 variations from each of the three images, the result was manually evaluated considering its respective ground truth. The crop lines were classified in three groups: a) in Green segments of the plantation row correctly classified by the algorithm; b) in Red were represented the segments not identified by the algorithm that actually are part of the plantation row; and c) in Blue the segments identified by the algorithm that are not part of the plantation row. Fig. 6-c,d shows the ground truth generated prior to the application of the proposed algorithm. Fig. 7 shows the manual classification procedure after.
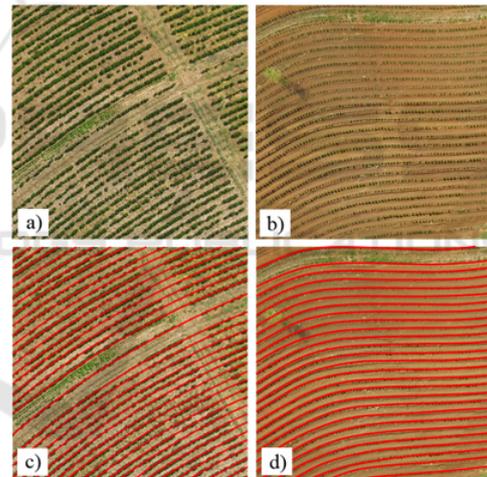

Figure 6: Data Set Example: (a) and (b) are two original images; (c) and (d) represent the images after ground truth definition.

The values presented on table 1 were combined generating 36 combinations of the parameters α, β and γ. For the images processed under each of such parameter set, the accuracy rate was obtained by the equation (3). The values of true-positive, true-negative, false-positive and false-negative were obtained manually by direct measurements against the ground truth. A example of this process is presented on Fig. 7.

$$accuracy = \frac{TP}{TP + FN + FP} \qquad (3)$$

In order to measure the accuracy rate, the Jaccard

Table 1: Values tested for the variables used in the proposed algorithm.

(β)	(α)	(γ)
50	0%	1.5
100	25%	2.0
150	48%	2.5
200	-	-

Coefficient was used, since this index disregard the true-negative values, what in this case, represents all the image area with no crop lines, which could compromise the results.
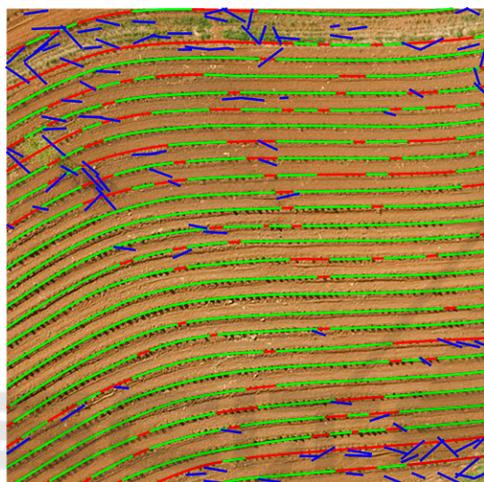

Figure 7: Accuracy Analysis Example: red line = False-Negative, blue line = False-Positive and green lines = True-Positive.

The accuracy rate achieved in the experiments was associated with which one of the parameters evaluated. The chart presented on Fig. 8 relate the accuracy rate with the denoising index. According to data represented on this graphic, is impossible to determine a relationship between the accuracy rate and the denoising index.

However, by considering the relationship between the tile size and the overlap rate with the accuracy rate, the dependence between this values was made clear. Especially when considered the values of overlap rate (Fig. 9-a). Higher values of overlap rate produce better accuracy scores. Experimentally, overlaps larger than 48% haven't succeed in improve the results.

A curious behavior can be observed regarding the tile size defined by parameter (β). It is possible to see on Fig. 9-b, that the results obtained fluctuates. To understand this result is important to realize that each value of β tested was combined with two others parameters as represented on Table 1. Thus, were generated and tested nine sets of parameters for each
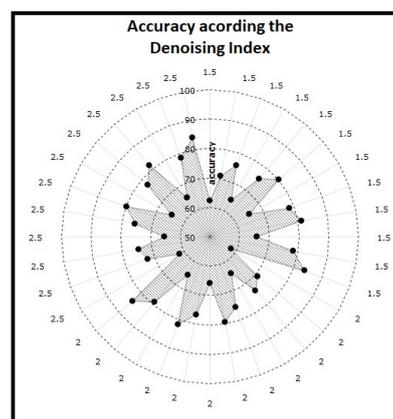

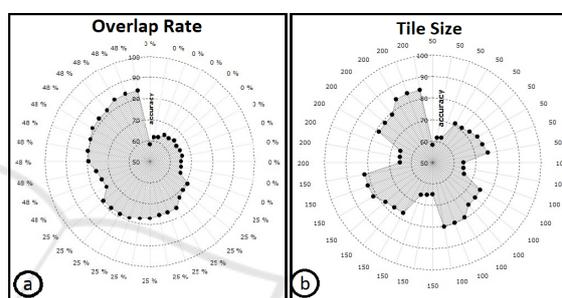Figure 8: Results obtained with the denoising algorithm.

Figure 9: Polar plot of (a) Accuracy×Overlap rate, and (b) Accuracy×Tile size.

value of β. For the design of the chart represented on 9-b the data were sorted by the values of β as the first criteria and by the overlap rate as the second criteria. Thus is possible to realize that for the same values of β the proposed algorithm achieve different accuracy values and they are totally dependent of the overlap rate value. The best results were obtained using $\alpha = 0.48$ and $\beta = 200$. Those values were then used to apply the method on five other images in order to test its reproductibility. It was possible to certify that the average accuracy rate was maintained, with the results on Table 2.

4 CONCLUSION

In this work were explored the application of Hough Transform to extract plantation lines on UAV imaged crop fields. In order to make it feasible were proposed to tile the entire image into overlapped windows. This approach accomplished to limit the information inside each window to lines of manageable size which can be considered locally straight making viable the use of the Hough Transform. The overlapping windows has shown to be a necessity in order to avoid discontinuities in the plantation lines.

Also a method were proposed to treat the unaligned lines generated by the proposed algorithm. These lines were considered and treated in this work as noise. Based on empiric analysis the technique developed prove itself a promising strategy to solve the problem. It suggest future works in order to analyze effectively the denoising algorithm proposed and assess quantitatively their effectiveness.

Another interesting byproduct of the proposed approach is the possibility of parallelization. Each window is independent from one another making it ideal to be implemented as a divide and conquer approach. Considering that in production the size of the imaged fields can be really large leading to possibly gigabytes of image data, the post flight processing can take considerable time. By parallelizing the process, the UAV companies doing agricultural survey are enabled to deliver the final processing result in a fraction of the usual time.

ACKNOWLEDGMENT

REFERENCES

AUVSI (2013). The economic impact of unmanned aircraft systems integration in the united states march. Economic report, Association for Unmanned Vehicle Systems International, Washington DC,.

Ballard, D. H. (1981). Generalizing the hough transform to detect arbitrary shapes. *Pattern Recognition*, 13(Issue 2):111–122. doi:10.1016/0031-3203(81)90009-1.

Blackmer, T. M. and Schepers, J. S. (1996). Aerial photography to detect nitrogen stress in corn. *Journal of Plant Physiology*, 148:440–444. doi:10.1016/S0176-1617(96)80277-X.

García-Santillán, I., Guerrero, J. M., Montalvo, M., and Pajares, G. (2017). Curved and straight crop row detection by accumulation of green pixels from images in maize fields. *Precision Agriculture*. doi:10.1007/s11119-016-9494-1.

Hough, P. (1962). Method and Means for Recognizing Complex Patterns. U.S. Patent 3.069.654.

Illingworth, J. and Kittler, J. (1988). A survey of the hough transform. *Computer Vision, Graphics, and Image Processing*, 44(Issue 1):87–116. doi:10.1016/S0734-189X(88)80033-1.

Kataoka, T., Kaneko, T., Okamoto, H., and Hata, S. (2003). Crop growth estimation system using machine vision. In *Advanced Intelligent Mechatronics*. doi:10.1109/AIM.2003.1225492.

Lee, I.-K. (2000). Curve reconstruction from unorganized points. *Computer Aided Geometric Design*, 17(Issue 2):161–177. doi:10.1016/S0167-8396(99)00044-8.

Leemans, V. and Destain, M.-F. (2006). Line cluster detection using a variant of the hough transform for culture row localisation. *Image and Video Computing*, 24:541–550.

Ramesh, K. N., Omkar, N., Meenavathi, M. B., and Rekha, V. (2016). Detection of row in agricultural crop images acquired by remore sensing from a uav. *International Journal of Graphics and Signal Processing*, 11:25–31.

Ronghua, J. and Lijun, L. (2011). Crop-row detection algorithm based on random hough transformation. *Mathematical and Computer Modelling*, 54:1016–1020.

Sankaran, S., Khot, L. R., et al. (2015). Low-altitude, high-resolution aerial imaging systems for row and field crop phenotyping: A review. *European Journal of Agronomy*, 70:112–123. doi:10.1016/j.eja.2015.07.004.

Søgaard, H. T. and Olsen, H. J. (2003). Determination of crop rows by image analysis without segmentation. *Computers and Electronics in Agriculture*, 38(Issue 2):141–158. doi:10.1016/S0168-1699(02)00140-0.

Turner, J., Kenkel, P., Holcomb, R. B., and Arnall, B. (2016). Economic potential of unmanned aircraft in agricultural and rural electric cooperatives. In *2016 Annual Meeting of Southern Agricultural Economics Association*, number 230047, page 18, San Antonio, Texas.